ACS OMEGA

http://pubs.acs.org/journal/acsodf

Article

Twist-Dependent Tuning of Excitonic Emissions in Bilayer WSe_2

Prahalad Kanti Barman,[#] Pranshoo Upadhyay,[#] Ramesh Rajarapu, Sharad Kumar Yadav, Latha K. V. P., Meenakshisundaram N., and Pramoda K. Nayak*

Cite This: *ACS Omega* 2022, 7, 6412−6418

Read Online

ACCESS | Metrics & More | Article Recommendations | Supporting Information

ABSTRACT: Monolayer (ML) transition metal dichalcogenides (TMDCs) have been rigorously studied to comprehend their rich spin and valley physics, exceptional optical properties, and ability to open new avenues in fundamental research and technology. However, intricate analysis of twisted homobilayer (t-BL) systems is highly required due to the intriguing twist angle (t-angle)-dependent interlayer effects on optical and electrical properties. Here, we report the evolution of the interlayer effect on artificially stacked BL WSe_2, grown using chemical vapor deposition (CVD), with t-angle in the range of $0 \leq \theta \leq 60°$. Systematic analyses based on Raman and photoluminescence (PL) spectroscopies suggest intriguing deviations in the interlayer interactions, higher-energy exciton transitions (in the range of ∼1.6−1.7 eV), and stacking. In contrast to previous observations, we demonstrate a red shift in the PL spectra with t-angle. Density functional theory (DFT) is employed to understand the band-gap variations with t-angle. Exciton radiative lifetime has been estimated theoretically using temperature-dependent PL measurements, which shows an increase with t-angle that agrees with our experimental observations. This study presents the groundwork for further investigation of the evolution of various interlayer excitons and their dynamics with t-angle in homobilayer systems, critical for optoelectronic applications.

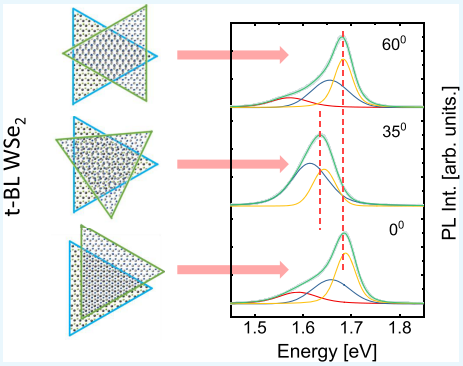

1. INTRODUCTION

Van der Waals (vdW) coupling is emerging as a powerful method to engineer and tailor the physical properties of atomically thin two-dimensional (2D) materials.[1−4] Transition metal dichalcogenides (TMDCs) with the chemical formula MX_2 (M = W, Mo, and so on and X = S, Se, or Te) are a class of 2D materials consisting of predominantly vdW-coupled atomically thin layers and exhibiting interesting optical properties governed by their structural symmetry[5,6] and interlayer coupling,[7−9] which are highly susceptible to stacking. As these ultrathin materials are very sensitive to the dielectric environment and interlayer interactions, understanding these interactions is a key scientific challenge for building functional homo- or heterojunction devices and novel hybrid 2D materials.[10] In the evolving era of twistronics, twisted vdW hetero- and homostructures have demonstrated a plethora of novel phases and functionalities.[11−13] They have many advantages over conventional heterostructures including atomically sharp interfaces, no interdiffusion of atoms, and no lattice parameter constraints.[2]

Synthesis of monolayer (ML)-to-few-layer TMDCs using chemical vapor deposition (CVD) has already been reported by many research groups,[14−17] and their layer-dependent electronic, optical, and vibrational properties have also been investigated in sufficient detail.[18−23] In the last few years, there has been a surge of interest in the heterojunction of these ML TMDCs.[24−28] Owing to a large number of TMDCs being available, a variety of combinations have been implemented in the literature to observe several unique intriguing optical and electrical features.[29−32] This leads to a strong motivation to understand how the twist affects interlayer interactions and the excitonic level properties in these materials. However, limited investigations are available on homobilayer systems, which are essential for emerging applications in twistronics, spintronics, valleytronics, and optoelectronics. A few reports on homobilayers, such as Van Der Zande et al.[10] showing optical and vibrational properties of mechanically stacked t-BL MoS_2 bilayers, Ji et al.[33] showing changes in the photoluminescence (PL) pathway in t-BL WS_2, and Scuri et al.[34] demonstrating gate-controlled valley dynamics in t-BL WSe_2, can be found. The limitations in the study on homo-t-BL TMDCs are, so far, due to the difficulties involved in the transfer process and challenges involved in determining the exciton dynamics, the exact origin of PL peaks, and evolution of interlayer interactions with t-angle.

In this paper, we demonstrate an intriguing effect of t-angle on the exciton−trion transition and the evolution of interlayer coupling in t-BL WSe_2. We predict the presence of interlayer excitations for different t-angles in the range of $0 \leq \theta \leq 60°$.

Received: December 22, 2021
Accepted: January 28, 2022
Published: February 11, 2022

https://doi.org/10.1021/acsomega.1c07219
ACS Omega 2022, 7, 6412−6418

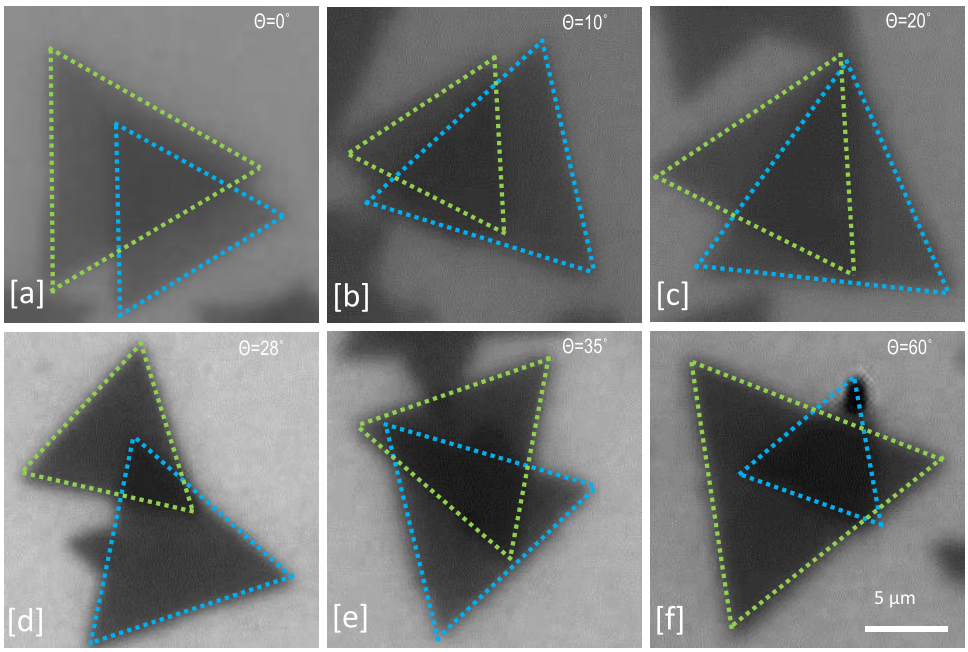

Figure 1. [a–f] OM images of t-BL WSe_2 samples on SiO_2/Si substrate with different t-angles indicated by θ.

Artificially stacked t-BLs on SiO_2/Si substrate with different t-angles demonstrate tunable PL emissions including a drastic red shift at room temperature (RT) PL and competition between different excitonic emission peaks with increasing t-angle relative to 0 and 60°. The observed variations provide evidence of a t-angle-dependent change in stacking symmetry, leading to variation in interlayer coupling strength and interlayer excitons (IEs) in our t-BL systems.

2. METHODS

The ML WSe_2 flakes on a sapphire substrate were synthesized using a low-pressure chemical vapor deposition (LPCVD) method similar to that in our earlier report.[35] The as-grown ML WSe_2 flakes were transferred onto a 300 nm SiO_2/Si substrate using a PMMA-assisted transfer process.[35] The transfer process was repeated another time on WSe_2/(SiO_2/Si) prepared earlier to synthesize BL WSe_2 flakes. To enhance the coupling between the two layers, the samples were annealed in vacuum (<0.1 Pa) with a flow of Ar gas (100 sccm) at 300 °C for 12 h. BL flakes with selected twist angles ranging from $0 \leq \theta \leq 60°$ were chosen for Raman and PL analyses.

Optical microscopy (OM) images were taken on an Olympus (model no. BX51RF) microscope, with a 100X objective lens with NA ∼ 0.95. Both low-frequency (LF) and high-frequency (HF) Raman measurements were performed at RT using a confocal Raman system (Wi-Tech, model no. Alpha 300 M+) with backscattering geometry under 488 nm laser excitation. The laser was focused to a spot size of ∼1 μm on the sample, obtained with 1800 gr/mm grating. PL spectra of WSe_2 flakes prepared on 300 nm SiO_2/Si substrates were obtained using a high-resolution μRaman spectrometer (LabRam 800, Horiba Jobin Yvon) in backscattering geometry. Green laser (514 nm) and red laser (632 nm) were used as excitation sources for RT measurement, which were focused to a spot size of ∼1 μm on the sample, obtained with 600 gr/mm grating. Low-temperature (LT) PL measurement was carried out with 488 nm laser excitation with the same configuration as mentioned before. The laser power was kept low (∼50 μW) to avoid local heating.

3. RESULTS AND DISCUSSION

In this work, we consider various BL WSe_2 samples with different t-angles in the range of $0 \leq \theta \leq 60°$ as shown in Figure 1, and their corresponding schematics are given in Figure S1 (Supporting Information). The thickness of vertically stacked ML flakes is confirmed by AFM measurements, illustrated in Figure S2 (Supporting Information), and found to be consistent with earlier reports.[36−38] LF RT Raman spectra of t-BL WSe_2 samples shown in Figure 2 reveal shear (S) and layer breathing (LB) modes in symmetric 0° (60°) stacking at ∼19 (∼16.5) cm^{-1} and ∼33 (∼28) cm^{-1}, respectively, analogous to the MoX_2 system.[39,40] LB modes in symmetric stacking are addressed as LB1. Here, 0 and 60° are shifted with respect to each other. This is in accordance with their difference in the stacking orders (R and H, respectively). Decrease (Increase) in the intensity of S (LB1) mode from 60 to 0° and greater separation of the two peaks for 0° confirm the different polytypes,[41,42] while an extra LB (called LB2) mode emerges for asymmetric stacking with no evidence of S mode, confirming the absence of restoring forces in intermediate t-angles. The emergence of the LB2 mode may be attributed to the misaligned structure in the asymmetric stackings. On examining the variation of LB1 with t-angle, softening of the mode for asymmetric stackings is noted, indicating weaker interlayer coupling. In contrast, HF RT Raman spectra do not show considerable shifts with t-angle, eliminating the presence of significant strain in the samples.

HF Raman spectra are separated into two parts, as shown in Figure S3a,b. Intralayer E^1_{2g} [Γ] (∼248.7 cm^{-1}) and A_{1g} [Γ] (∼251.5 cm^{-1}) modes, seldom resolved together due to excitation polarization dependency,[43] are indicated along with a higher-order resonance 2LA[M] mode in Figure S3a. Moreover, improved interlayer coupling due to annealing of artificially stacked samples is confirmed from the emergence of B^1_{2g} [Γ] mode at ∼308 cm^{-1} in t-BL samples and its absence in

https://doi.org/10.1021/acsomega.1c07219
ACS Omega 2022, 7, 6412−6418

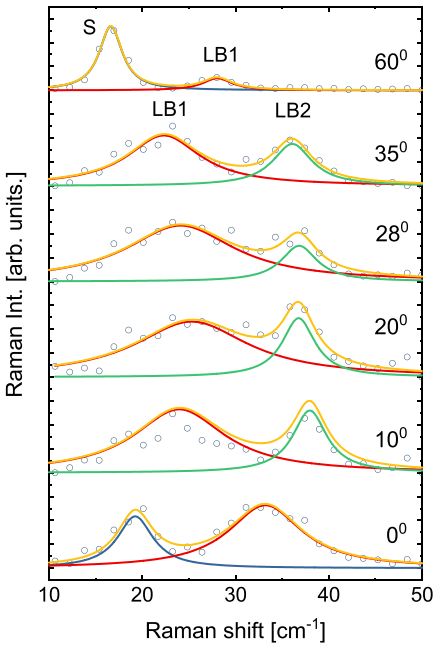

Figure 2. LF Raman spectra of t-BL WSe_2 with different t-angles in the range of $0 \leq \theta \leq 60°$. Shear (S) and layer breathing (LB1 and LB2) modes are marked.

ML samples, as shown in Figures S3b and S4. Also, the intensity variation of this mode with t-angle agrees with the conclusion drawn from the softening of the LB1 mode regarding the interlayer interactions. In addition, its higher intensity for 60° than 0° t-BL confirms the stronger interlayer coupling in the former owing to its H-type stacking as discussed earlier.

Furthermore, RT PL spectra are depicted in Figure 3a for ML and t-BL WSe_2 samples to analyze t-angle dependency on excitonic transition. ML WSe_2 shows a sharp peak at ∼1.68 eV, attributed to direct-band-gap (BG) K−K transition. The asymmetric nature of the PL envelope of ML WSe_2 indicates contributions from neutral exciton (AX^0) and charged exciton (AX^-) separated by ∼28−32 meV, which is in good agreement with earlier reports.[44] The narrow full width at half-maximum (FWHM) of ∼41 meV for AX^0 gives an inference of highly crystalline WSe_2 flakes with minimal defect states. The wider spectrum in BL samples is the result of several momentum dark exciton states and trion states in close proximity to the highest-energy bright exciton peak. The additional peak (indirect in nature) at ∼1.58 eV (0° t-BL) is regarded as a momentum dark exciton or a localized exciton and labeled *IX*. *IX* is apparent for stable stackings at 0 and 60° but not for asymmetric stackings, indicating a direct BG nature for the latter. Interestingly, an unintuitive red shift in PL is observed for intermediate t-angles compared to stable stackings, as illustrated in Figure 3b. Contradictorily, in the literature, several earlier works have reported a blue shift in PL with increasing t-angles in BL WSe_2.[45,46,45,46] But these studies carried out at cryogenic temperatures (<10 K) are for momentum indirect Q−K or Q−Γ emissions at lower energies (∼1.5−1.6 eV). As opposed to Mo-based TMDs,[47−49] the direct emission peak near ∼1.7 eV in WSe_2 is strongly quenched at lower temperatures due to the presence of lower-lying dark exciton states (see Supporting Information, Figure S5). This makes it difficult to resolve the peaks near AX^0 even at low temperatures. However, the red shift in the direct exciton peak of W-based TMDs is evident in recent reports by Zheng et al.[50] and Ji et al.[33] Also, in the report by Merkl et al.,[46] the K−K peak is seen to shift closer to the Q−K peak with increasing t-angles at 4 K in WSe_2. Although the results in these reports indicate such an interesting feature, a discussion on the origin of such a shift is clearly missing.

For confirmation, RT PL measurements were repeated using a different laser excitation (514 nm) on all t-angles, and the same trend was found, as shown in Figure S6 (Supporting Information). Initially, one may come up with two possible explanations of either strain-induced (due to twist) red shift or K−K band-gap reduction. However, on the one hand, Raman measurements indicate the absence of any significant strain, and on the other hand, our density functional theory (DFT)

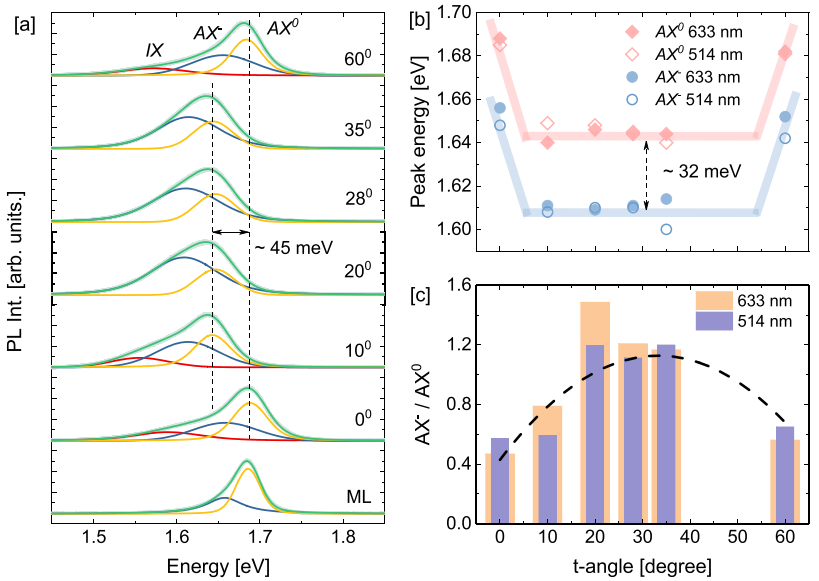

Figure 3. [a] RT PL spectra at 633 nm excitation for ML and t-BL-WSe_2 with different t-angles, respectively. [b] Peak position of AX^0 and AX^- with different t-angles. [c] Peak intensity ratio of trion and exciton with different t-angles.

https://doi.org/10.1021/acsomega.1c07219
ACS Omega 2022, 7, 6412−6418

calculations (details in Supporting Information Note 1) show the negligible effect of t-angle on $K-K$ BG as shown in Figure 4. At 60 and 21.78° (chosen to reduce computational

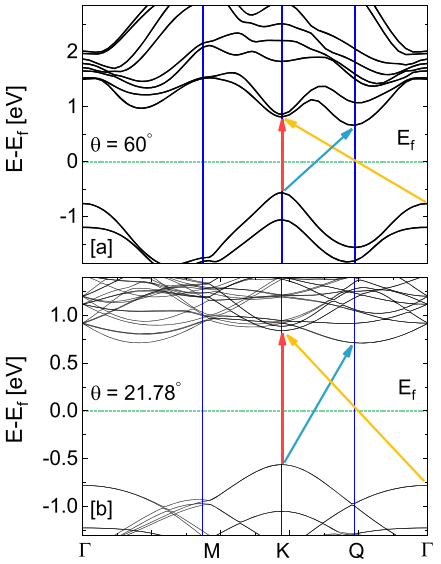

Figure 4. DFT calculated band structure of t-BL WSe_2 for 60° [a] and 21.78° [b]. Red arrows indicate the direct BG transitions. Blue and yellow arrows correspond to the indirect BG transitions.

complexity) t-angles, a similar BG of ∼1.3 eV is obtained at K valley with merely a ∼9 meV difference. For 0 and 27.79°, refer to the Supporting Information Figure S7. This is widely expected in group VI-based TMDs due to the major contributions from d orbitals of transition metal at K point, leading to comparatively weaker interlayer coupling at the band edge state. Further, the AX^0 peak blue-shifts from ML to symmetrically stacked BL WSe_2 as shown in Figures 3a and S6, which is significant in LT PL (Figure 5a). This will be an unexpected result if we consider the AX^0 peak to be solely from intralayer A exciton emission. Here, we consider AX^0 in t-BL samples not to be from $K-K$ intralayer exciton owing to the red shift with t-angle and blue shift from ML to BL. This strongly indicates the presence of interlayer excitons (IEs). As explained earlier, the difficulty in resolving these peaks even at cryogenic temperatures makes it more challenging to determine the exact origin. However, we try to present an intuitive and logical explanation here.

First, due to the contributions from W d orbitals at K/K' point in BL WSe_2, the interlayer hopping amplitude of both the electrons and holes is less than the spin-splitting at the conduction and valence bands (specifically for H stacking), respectively. This restricts the carriers to a single layer at the K point of the Brillouin zone.[48,51] However, this restriction is valid only at the band edge K point of the Brillouin zone and not at a point close to K.[30] Owing to the finite momentum of the incident photon, the excitons can be excited at a position slightly away from the band edge state. Das et al.[52] provide details on the finite probability of formation and emission of this direct interlayer exciton. Hence, for the case of symmetric stackings (0 and 60° t-BL), the presence of momentum direct interlayer exciton at K can be considered. As the binding energy of interlayer exciton is less than that of intralayer exciton and the $K-K$ electronic BG does not have a considerable variation, the blue shift of the AX^0 peak observed from ML to BL is justified. Also, a difference in the peak position of AX^0 between 0 and 60° t-BL, shown in the PL spectra, can be explained using the deviation in spin-splitting and spin-valley locking of interlayer excitons in the two symmetrically different systems.[30] The formation of direct interlayer exciton at K occurs from the upper (lower) conduction band minimum in 0° (60°) t-BL WSe_2. However, justification for the red shift in the AX^0 peak with t-angle is still needed. Higher interlayer separation and momentum mismatch in the asymmetric stackings indicate lower binding energy of the interlayer exciton, as compared to symmetric stackings. This should, in general, lead to a blue shift in the peak position with t-angle, the inverse of the observed variation.

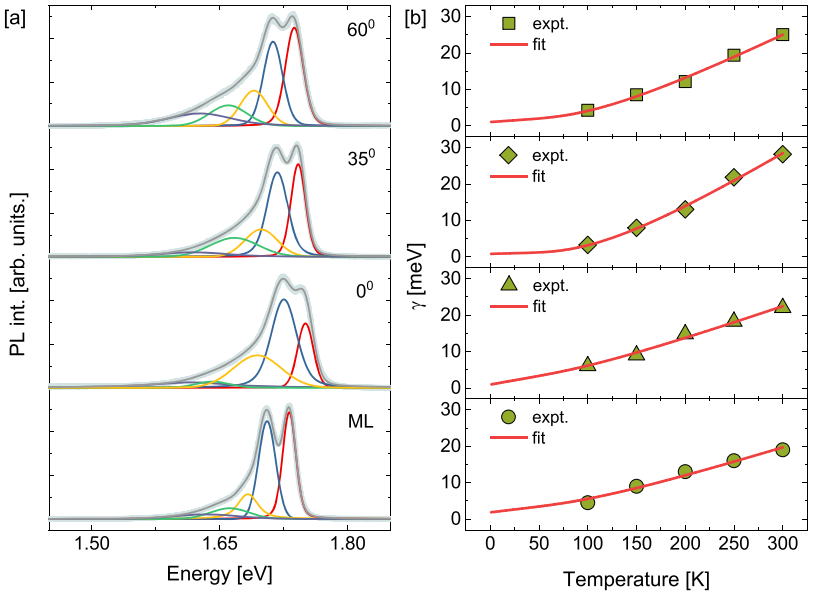

Figure 5. [a] PL spectra at 100 K and 488 nm excitation for ML and t-BL-WSe_2 with angles 0, 35, and 60°, respectively. [b] Lorentzian FWHM for AX^0 is extracted from Voigt profile fitting done on the PL spectra obtained at various temperatures for ML and t-BL flakes.

https://doi.org/10.1021/acsomega.1c07219
ACS Omega 2022, 7, 6412−6418

Earlier theoretical investigations on interlayer excitons in BL WSe_2 indicate the presence of several momentum dark exciton states ($K-\Gamma$ and $K-K'$) in close proximity to the $K-K$ transition (<~60 meV) peak that remain unresolved to date in experiments. Moreover, spin-splitting in K valley leads to two different indirect $K-\Gamma$ excitons that are shown to be red-shifted with respect to $K-K$ exciton by ~40 and ~100 meV.[53] Interestingly, the peak position of AX^0 does not vary for the intermediate t-angles and is approximately ~45 meV red-shifted from that of symmetric stackings. We assume the AX^0 peak in asymmetric stackings to be from the phonon-assisted emission of $K-\Gamma$ excitons with the electrons in the upper conduction band minimum at K valley. But again, intervalley scattering of holes in WSe_2 is considered to be forbidden due to large momentum mismatch and spin orbit splitting at K or K' valleys. However, as explained earlier, we have carriers near to but not exactly at K point, which makes this scattering to be allowed in nature. Importantly, this scattering is more prominent for thermally excited carriers, i.e., at RT. This is precisely our observation. RT PL spectra show a significant red shift from symmetric to asymmetric stacking when compared to those of LT PL. Furthermore, with the increase in interlayer separation and momentum mismatch, the $K-K$ transition is expected and observed to drastically quench. However, due to delocalization of the holes at the zone center, we have significant contributions from the momentum dark $K-\Gamma$ excitons for intermediate t-angles.

Next, the energy of the peak labeled IX (~100 meV red-shifted from $K-K$), observed in the symmetric stackings, lies close to the expected $K-\Gamma$ excitons with the electrons in lower conduction band minimum at K valley. The intensity of the IX peaks is observed to drastically quench in the asymmetric stackings, resembling a competition between the two $K-\Gamma$ excitons. Similarly, in Figure 3c, competition in the intensity of AX^- and AX^0 peaks is evident with t-angle. Also, AX^- energy shows a similar red shift as discussed earlier. This suggests the interlayer nature of the peak with contributions from K valley. The exact nature of the AX^- and IX peaks requires further investigation, which is out of the scope of this work.

Now, we attempt to address exciton dynamics to some extent using the temperature-dependent steady-state PL spectra (Figure S8, Supporting Information). Comprehending radiative recombination processes in TMDCs is challenging and requires precise time-resolved measurements and pump–probe measurements. Also, a complex technique such as four-wave mixing spectroscopy[54] needs to be employed for the determination of homogeneous and inhomogeneous components. Therefore, it is always beneficial to have a theoretical approach for estimating the value of a desired observable that requires an intricate experimental setup for its determination. For radiative lifetime variation with t-angle, a specific approach (Supporting Information Note 2) involving temperature-dependent homogeneous line width (γ) is used. It should be noted that this method is suitable only for the most significant peak (AX^0 in our case), as other peaks are mostly dominated by inhomogeneous broadening. Figure 5a demonstrates the deconvoluted peaks at 100 K for ML and t-BL WSe_2 samples. The significant blue shift observed in moving from ML to symmetric t-BL is unusual and only indicates the existence of interlayer excitons as discussed earlier. Here, γ of the AX^0 peak (in red) is extracted at temperatures ranging from 100 to 300 K (shown in Figure 5b) and fitted with Rudin's function[55] to obtain γ at 0 K, needed for lifetime estimation (refer Supporting Information Note 2). The radiative lifetime calculated for AX^0 at RT for ML (~1.2 ns) and t-BL (0, 35, and 60°) samples (~4.4, ~5.2, and ~4.1 ns, respectively) show a longer lifetime in BL, confirming the indirect nature of excitons in momentum and/or real space. The lifetime evaluated for the ML indicates a slower relaxation channel that dominates at RT[47] and a fast relaxation process that is predominant at low temperatures (~400 fs for ML and ~600–800 fs for t-BL at 0 K). However, our focus is based on trends rather than the actual values obtained from the theoretical approximations. Previous reports show improved overall lifetime in BL systems compared to ML due to either trion contribution[30] or indirect excitons. However, in our analysis, we observe an increase in the lifetime of AX^0 alone, discarding the role of AX^-. Also, the longest lifetime of AX^0 obtained for the misaligned stacking (35°) agrees with the transition from $K-K$ to $K-\Gamma$ excitons, as detailed above. $K-K$ is momentum direct for the case of symmetric stackings yet has a longer lifetime compared to intralayer excitons due to dielectric screening and spatial misalignment. But for other t-angles, the IEs at play are momentum indirect in nature ($K-\Gamma$) and are further spatially separated, resulting in the suppression of nonradiative relaxation channels and improvement in radiative lifetimes. Hence, a longer radiative lifetime of AX^0 is observed with a red shift in its peak position due to twists relative to stable stackings. These intriguing observations demand further intense investigations into theoretical and experimental aspects to fully comprehend twisted bilayer systems.

4. CONCLUSIONS

In this work, we present various experimental observations in Raman and PL spectra highlighting t-angle dependency in the interlayer coupling, nature of BGs, and interlayer excitons. One major observation was the red shift in PL spectra from symmetric to asymmetric stacking in t-BL WSe_2, prominent at RT. Possible explanations for this observation were made corroborating with the existing literature and DFT calculations. Evolution of the interlayer nature in the highest-energy peak from 1L to BL was predicted. Deviations in the interlayer excitons and radiative lifetimes were observed with the variation of stacking symmetry arising from the twist. The higher-energy PL peaks in W-based TMDCs tend to quench with lowering of temperature, increasing the complexity of resolving the peaks close to this energy. Hence, this work demands more rigorous theoretical investigations on twist-dependent evolution of trions and high energy interlayer excitons in these homobilayer systems.

■ ASSOCIATED CONTENT

Supporting Information

The Supporting Information is available free of charge at https://pubs.acs.org/doi/10.1021/acsomega.1c07219.

AFM image; HF Raman spectra; Raman shift after postannealing; PL spectra at 514 nm excitation; temperature variation of PL spectra; additional band structure; note for band structure and exciton lifetime calculation (PDF)

■ AUTHOR INFORMATION

Corresponding Author

Pramoda K. Nayak − *Department of Physics, Indian Institute of Technology Madras, Chennai 600 036, India; 2D*

https://doi.org/10.1021/acsomega.1c07219
ACS Omega 2022, 7, 6412−6418

Materials Research and Innovation Group and Micro Nano and Bio-Fluidics Group, Indian Institute of Technology Madras, Chennai 600036, India; orcid.org/0000-0002-2569-0517; Email: pnayak@iitm.ac.in

Authors

Prahalad Kanti Barman − *Department of Physics, Indian Institute of Technology Madras, Chennai 600 036, India; 2D Materials Research and Innovation Group, Indian Institute of Technology Madras, Chennai 600036, India*

Pranshoo Upadhyay − *Department of Physics, Indian Institute of Technology Madras, Chennai 600 036, India; 2D Materials Research and Innovation Group, Indian Institute of Technology Madras, Chennai 600036, India;* orcid.org/0000-0001-9133-1208

Ramesh Rajarapu − *Department of Physics, Indian Institute of Technology Madras, Chennai 600 036, India; 2D Materials Research and Innovation Group, Indian Institute of Technology Madras, Chennai 600036, India*

Sharad Kumar Yadav − *Department of Physics, Indian Institute of Technology Madras, Chennai 600 036, India; Micro Nano and Bio-Fluidics Group, Indian Institute of Technology Madras, Chennai 600036, India*

Latha K. V. P. − *Department of Physics, Pondicherry University, Pondicherry 605014, India*

Meenakshisundaram N. − *Department of Physics, Vivekananda College, Madurai 625234, India*

Complete contact information is available at: https://pubs.acs.org/10.1021/acsomega.1c07219

Author Contributions

#P.K.B. and P.U. contributed equally to this work.

Notes

The authors declare no competing financial interest.

■ ACKNOWLEDGMENTS

P.K.N. acknowledges the financial support from the Department of Science and Technology, Government of India (DST-GoI), with sanction Order No. SB/S2/RJN-043/2017 under the Ramanujan Fellowship. This work was also partially supported by the Indian Institute of Technology Madras for the 2D Materials Research and Innovation Group and Micro-Nano and Bio-Fluidics Group under the funding for Institutions of Eminence scheme of Ministry of Education, GoI [Sanction. No: 11/9/2019-U.3 (A)]. L.K.V.P. and M.N. thank DST-SERB for financial support through project no. SB/FTP/PS-142/2013 and project no. YSS/2015/000954.

■ REFERENCES

(1) Geim, A. K.; Grigorieva, I. V. Van Der Waals Heterostructures. *Nature* **2013**, *499*, 419−425.

(2) Fang, H.; Battaglia, C.; Carraro, C.; Nemsak, S.; Ozdol, B.; Kang, J. S.; Bechtel, H. A.; Desai, S. B.; Kronast, F.; Unal, A. A.; et al. Strong Interlayer Coupling in van Der Waals Heterostructures Built from Single-Layer Chalcogenides. *Proc. Natl. Acad. Sci. U.S.A.* **2014**, *111*, 6198−6202.

(3) Lim, H.; Yoon, S. I.; Kim, G.; Jang, A. R.; Shin, H. S. Stacking of Two-Dimensional Materials in Lateral and Vertical Directions. *Chem. Mater.* **2014**, *26*, 4891−4903.

(4) Gao, G.; Gao, W.; Cannuccia, E.; Taha-Tijerina, J.; Balicas, L.; Mathkar, A.; Narayanan, T. N.; Liu, Z.; Gupta, B. K.; Peng, J.; et al. Artificially Stacked Atomic Layers: Toward New van Der Waals Solids. *Nano Lett.* **2012**, *12*, 3518−3525.

(5) Xiao, D.; Liu, G. B.; Feng, W.; Xu, X.; Yao, W. Coupled Spin and Valley Physics in Monolayers of MoS2 and Other Group-VI Dichalcogenides. *Phys. Rev. Lett.* **2012**, *108*, No. 196802.

(6) Yao, W.; Xiao, D.; Niu, Q. Valley-Dependent Optoelectronics from Inversion Symmetry Breaking. *Phys. Rev. B* **2008**, *77*, No. 235406.

(7) Mak, K. F.; Lee, C.; Hone, J.; Shan, J.; Heinz, T. F. Atomically Thin MoS2: A New Direct-Gap Semiconductor. *Phys. Rev. Lett.* **2010**, *105*, No. 136805.

(8) Zhao, W.; Ribeiro, R. M.; Toh, M.; Carvalho, A.; Kloc, C.; Castro Neto, A. H.; Eda, G. Origin of Indirect Optical Transitions in Few-Layer MoS2, WS2, and WSe2. *Nano Lett.* **2013**, *13*, 5627−5634.

(9) Zhang, Y.; Chang, T. R.; Zhou, B.; Cui, Y. T.; Yan, H.; Liu, Z.; Schmitt, F.; Lee, J.; Moore, R.; Chen, Y.; et al. Direct Observation of the Transition from Indirect to Direct Bandgap in Atomically Thin Epitaxial MoSe2. *Nat. Nanotechnol.* **2014**, *9*, 111−115.

(10) Van Der Zande, A. M.; Kunstmann, J.; Chernikov, A.; Chenet, D. A.; You, Y.; Zhang, X.; Huang, P. Y.; Berkelbach, T. C.; Wang, L.; Zhang, F.; et al. Tailoring the Electronic Structure in Bilayer Molybdenum Disulfide via Interlayer Twist. *Nano Lett.* **2014**, *14*, 3869−3875.

(11) Wang, S.; Cui, X.; Jian, C.; Cheng, H.; Niu, M.; Yu, J.; Yan, J.; Huang, W. Stacking-Engineered Heterostructures in Transition Metal Dichalcogenides. *Adv. Mater.* **2021**, *33*, No. 2005735.

(12) He, F.; Zhou, Y.; Ye, Z.; Cho, S. H.; Jeong, J.; Meng, X.; Wang, Y. Moiré Patterns in 2D Materials: A Review. *ACS Nano* **2021**, *15*, 5944−5958.

(13) Andersen, T. I.; Scuri, G.; Sushko, A.; De Greve, K.; Sung, J.; Zhou, Y.; Wild, D. S.; Gelly, R. J.; Heo, H.; Bérubé, D.; et al. Excitons in a Reconstructed Moiré Potential in Twisted WSe2/WSe2 Homobilayers. *Nat. Mater.* **2021**, *20*, 480−487.

(14) Chhowalla, M.; Shin, H. S.; Eda, G.; Li, L.-J.; Loh, K. P.; Zhang, H. The Chemistry of Two-Dimensional Layered Transition Metal Dichalcogenide Nanosheets. *Nat. Chem.* **2013**, *5*, 263−275.

(15) Huang, J. K.; Pu, J.; Hsu, C. L.; Chiu, M. H.; Juang, Z. Y.; Chang, Y. H.; Chang, W. H.; Iwasa, Y.; Takenobu, T.; Li, L. J. Large-Area Synthesis of Highly Crystalline WSe2 Monolayers and Device Applications. *ACS Nano* **2014**, *8*, 923−930.

(16) Shi, Y.; Li, H.; Li, L. J. Recent Advances in Controlled Synthesis of Two-Dimensional Transition Metal Dichalcogenides via Vapour Deposition Techniques. *Chem. Soc. Rev.* **2015**, *44*, 2744−2756.

(17) Sarma, P. V.; Patil, P. D.; Barman, P. K.; Kini, R. N.; Shaijumon, M. M. Controllable Growth of Few-Layer Spiral WS2. *RSC Adv.* **2016**, *6*, 376−382.

(18) Lee, C.; Yan, H.; Brus, L. E.; Heinz, T. F.; Hone, J.; Ryu, S. Anomalous Lattice Vibrations of Single- and Few-Layer MoS2. *ACS Nano* **2010**, *4*, 2695−2700.

(19) Wang, Q. H.; Kalantar-Zadeh, K.; Kis, A.; Coleman, J. N.; Strano, M. S. Electronics and Optoelectronics of Two-Dimensional Transition Metal Dichalcogenides. *Nat. Nanotechnol.* **2012**, *7*, 699−712.

(20) Berkdemir, A.; Gutiérrez, H. R.; Botello-Méndez, A. R.; Perea-López, N.; Elías, A. L.; Chia, C. I.; Wang, B.; Crespi, V. H.; López-Urías, F.; Charlier, J. C.; et al. Identification of Individual and Few Layers of WS_2 Using Raman Spectroscopy. *Sci. Rep.* **2013**, *3*, No. 1755.

(21) Nayak, P. K.; Yeh, C. H.; Chen, Y. C.; Chiu, P. W. Layer-Dependent Optical Conductivity in Atomic Thin WS2 by Reflection Contrast Spectroscopy. *ACS Appl. Mater. Interfaces* **2014**, *6*, 16020−16026.

(22) Barman, P. K.; Sarma, P. V.; Shaijumon, M. M.; Kini, R. N. High Degree of Circular Polarization in WS2 Spiral Nanostructures Induced by Broken Symmetry. *Sci. Rep.* **2019**, *9*, No. 2784.

(23) Mol, P. R.; Barman, P. K.; Sarma, P. V.; Kumar, A. S.; Sahu, S.; Shaijumon, M. M.; Kini, R. N. Anomalously Polarised Emission from a MoS2/WS2 heterostructure. *Nanoscale Adv.* **2021**, *3*, 5676−5682.

(24) Rivera, P.; Schaibley, J. R.; Jones, A. M.; Ross, J. S.; Wu, S.; Aivazian, G.; Klement, P.; Seyler, K.; Clark, G.; Ghimire, N. J.; et al.

Observation of Long-Lived Interlayer Excitons in Monolayer MoSe2-WSe2 Heterostructures. *Nat. Commun.* **2015**, *6*, No. 6242.
(25) Gong, Y.; Lin, J.; Wang, X.; Shi, G.; Lei, S.; Lin, Z.; Zou, X.; Ye, G.; Vajtai, R.; Yakobson, B. I.; et al. Vertical and In-Plane Heterostructures from WS2/MoS2 Monolayers. *Nat. Mater.* **2014**, *13*, 1135−1142.
(26) Kang, J.; Li, J.; Li, S. S.; Xia, J. B.; Wang, L. W. Electronic Structural Moiré Pattern Effects on MoS2/MoSe2 2D Heterostructures. *Nano Lett.* **2013**, *13*, 5485−5490.
(27) Furchi, M. M.; Pospischil, A.; Libisch, F.; Burgdörfer, J.; Mueller, T. Photovoltaic Effect in an Electrically Tunable Van Der Waals Heterojunction. *Nano Lett.* **2014**, *14*, 4785−4791.
(28) Lee, G. H.; Lee, C. H.; Van Der Zande, A. M.; Han, M.; Cui, X.; Arefe, G.; Nuckolls, C.; Heinz, T. F.; Hone, J.; Kim, P. Heterostructures Based on Inorganic and Organic van Der Waals Systems. *APL Mater.* **2014**, *2*, No. 092511.
(29) Chen, K.; Wan, X.; Wen, J.; Xie, W.; Kang, Z.; Zeng, X.; Chen, H.; Xu, J. Bin. Electronic Properties of MoS2-WS2 Heterostructures Synthesized with Two-Step Lateral Epitaxial Strategy. *ACS Nano* **2015**, *9*, 9868−9876.
(30) Alexeev, E. M.; Ruiz-Tijerina, D. A.; Danovich, M.; Hamer, M. J.; Terry, D. J.; Nayak, P. K.; Ahn, S.; Pak, S.; Lee, J.; Sohn, J. I.; et al. Resonantly Hybridized Excitons in Moiré Superlattices in van Der Waals Heterostructures. *Nature* **2019**, *567*, 81−86.
(31) Jin, C.; Regan, E. C.; Wang, D.; Iqbal Bakti Utama, M.; Yang, C. S.; Cain, J.; Qin, Y.; Shen, Y.; Zheng, Z.; Watanabe, K.; et al. Identification of Spin, Valley and Moiré Quasi-Angular Momentum of Interlayer Excitons. *Nat. Phys.* **2019**, *15*, 1140−1144.
(32) Shin, G. H.; Park, C.; Lee, K. J.; Jin, H. J.; Choi, S. Y. Ultrasensitive Phototransistor Based on WSe2-MoS2 van Der Waals Heterojunction. *Nano Lett.* **2020**, *20*, 5741−5748.
(33) Ji, H. G.; Solís-Fernández, P.; Erkllç, U.; Ago, H. Stacking Orientation-Dependent Photoluminescence Pathways in Artificially Stacked Bilayer WS2 Nanosheets Grown by Chemical Vapor Deposition: Implications for Spintronics and Valleytronics. *ACS Appl. Nano Mater.* **2021**, *4*, 3717−3724.
(34) Scuri, G.; Andersen, T. I.; Zhou, Y.; Wild, D. S.; Sung, J.; Gelly, R. J.; Bérubé, D.; Heo, H.; Shao, L.; Joe, A. Y.; et al. Electrically Tunable Valley Dynamics in Twisted WSe2/WSe2 Bilayers. *Phys. Rev. Lett.* **2020**, *124*, No. 217403.
(35) Nayak, P. K.; Horbatenko, Y.; Ahn, S.; Kim, G.; Lee, J. U.; Ma, K. Y.; Jang, A. R.; Lim, H.; Kim, D.; Ryu, S.; et al. Probing Evolution of Twist-Angle-Dependent Interlayer Excitons in MoSe2/WSe2 van Der Waals Heterostructures. *ACS Nano* **2017**, *11*, 4041−4050.
(36) Wen, J.; Wang, H.; Chen, H.; Deng, S.; Xu, N. Room-Temperature Strong Coupling between Dipolar Plasmon Resonance in Single Gold Nanorod and Two-Dimensional Excitons in Monolayer WSe2. *Chin. Phys. B* **2018**, *27*, No. 096101.
(37) Rong, Y.; Fan, Y.; Leen Koh, A.; Robertson, A. W.; He, K.; Wang, S.; Tan, H.; Sinclair, R.; Warner, J. H. Controlling Sulphur Precursor Addition for Large Single Crystal Domains of WS2. *Nanoscale* **2014**, *6*, 12096−12103.
(38) Xu, K.; Wang, Z.; Du, X.; Safdar, M.; Jiang, C.; He, J. Atomic-Layer Triangular WSe2 Sheets: Synthesis and Layer-Dependent Photoluminescence Property. *Nanotechnology* **2013**, *24*, No. 465705.
(39) Puretzky, A. A.; Liang, L.; Li, X.; Xiao, K.; Sumpter, B. G.; Meunier, V.; Geohegan, D. B. Twisted MoSe2 Bilayers with Variable Local Stacking and Interlayer Coupling Revealed by Low-Frequency Raman Spectroscopy. *ACS Nano* **2016**, *10*, 2736−2744.
(40) Quan, J.; Linhart, L.; Lin, M. L.; Lee, D.; Zhu, J.; Wang, C. Y.; Hsu, W. T.; Choi, J.; Embley, J.; Young, C.; et al. Phonon Renormalization in Reconstructed MoS2 Moiré Superlattices. *Nat. Mater.* **2021**, *20*, 1100−1105.
(41) O'Brien, M.; McEvoy, N.; Hanlon, D.; Hallam, T.; Coleman, J. N.; Duesberg, G. S. Mapping of Low-Frequency Raman Modes in CVD-Grown Transition Metal Dichalcogenides: Layer Number, Stacking Orientation and Resonant Effects. *Sci. Rep.* **2016**, *6*, No. 19476.
(42) Van Baren, J.; Ye, G.; Yan, J. A.; Ye, Z.; Rezaie, P.; Yu, P.; Liu, Z.; He, R.; Lui, C. H. Stacking-Dependent Interlayer Phonons in 3R and 2H MoS2. *2D Mater.* **2019**, *6*, No. 025022.
(43) Zhao, W.; Ghorannevis, Z.; Amara, K. K.; Pang, J. R.; Toh, M.; Zhang, X.; Kloc, C.; Tan, P. H.; Eda, G. Lattice Dynamics in Mono- and Few-Layer Sheets of WS2 and WSe2. *Nanoscale* **2013**, *5*, 9677−9683.
(44) Zhu, B.; Chen, X.; Cui, X. Exciton Binding Energy of Monolayer WS2. *Sci. Rep.* **2015**, *5*, No. 9218.
(45) Gao, Z.; Liu, Y.; Liu, H.; Qiu, C.; Zheng, S.; Liu, D. Tunable Exciton Radiative Recombination Lifetime in Twisted Bilayer Molybdenum Disulfide. *J. Phys. Chem. C* **2020**, *124*, 21123−21128.
(46) Merkl, P.; Mooshammer, F.; Brem, S.; Girnghuber, A.; Lin, K. Q.; Weigl, L.; Liebich, M.; Yong, C. K.; Gillen, R.; Maultzsch, J.; et al. Twist-Tailoring Coulomb Correlations in van Der Waals Homobilayers. *Nat. Commun.* **2020**, *11*, No. 2167.
(47) Zhang, X. X.; You, Y.; Zhao, S. Y. F.; Heinz, T. F. Experimental Evidence for Dark Excitons in Monolayer WSe_2. *Phys. Rev. Lett.* **2015**, *115*, No. 257403.
(48) Brem, S.; Lin, K. Q.; Gillen, R.; Bauer, J. M.; Maultzsch, J.; Lupton, J. M.; Malic, E. Hybridized Intervalley Moiré Excitons and Flat Bands in Twisted WSe2 bilayers. *Nanoscale* **2020**, *12*, 11088−11094.
(49) Wang, Z.; Chiu, Y. H.; Honz, K.; Mak, K. F.; Shan, J. Electrical Tuning of Interlayer Exciton Gases in WSe2 Bilayers. *Nano Lett.* **2018**, *18*, 137−143.
(50) Zheng, S.; Sun, L.; Zhou, X.; Liu, F.; Liu, Z.; Shen, Z.; Fan, H. J. Coupling and Interlayer Exciton in Twist-Stacked WS_2 Bilayers. *Adv. Opt. Mater.* **2015**, *3*, 1600−1605.
(51) Arora, A.; Nayak, P. K.; Bhattacharyya, S.; Maity, N.; Singh, A. K.; Krishnan, A.; Rao, M. S. R. Interlayer Excitonic States in MoSe2/MoS2 van Der Waals Heterostructures. *Phys. Rev. B* **2021**, *103*, No. 205406.
(52) Das, S.; Gupta, G.; Majumdar, K. Layer Degree of Freedom for Excitons in Transition Metal Dichalcogenides. *Phys. Rev. B* **2019**, *99*, No. 165411.
(53) Lindlau, J.; Selig, M.; Neumann, A.; Colombier, L.; Förste, J.; Funk, V.; Förg, M.; Kim, J.; Berghäuser, G.; Taniguchi, T.; et al. The Role of Momentum-Dark Excitons in the Elementary Optical Response of Bilayer WSe2. *Nat. Commun.* **2018**, *9*, No. 2586.
(54) Moody, G.; Kavir Dass, C.; Hao, K.; Chen, C. H.; Li, L. J.; Singh, A.; Tran, K.; Clark, G.; Xu, X.; Berghäuser, G.; et al. Intrinsic Homogeneous Linewidth and Broadening Mechanisms of Excitons in Monolayer Transition Metal Dichalcogenides. *Nat. Commun.* **2015**, *6*, No. 8315.
(55) Rudin, S.; Reinecke, T. L.; Segall, B. Temperature-Dependent Exciton Linewidths in Semiconductors. *Phys. Rev. B* **1990**, *42*, No. 11218.

https://doi.org/10.1021/acsomega.1c07219
ACS Omega 2022, 7, 6412−6418